Prof. Yu Huang
Key Lab of Aerosol Chemistry & Physics,
Institute of Earth Environment, Chinese Academy of Sciences, Xi'an, 710061, China
Tel./Fax: (86) 29-62336261
E-mail: huangyu@ieecas.cn

Jan. 31, 2019

Dear reviewer,

Revision for Manuscript acp-2018-935

We thank you very much for giving us the opportunity to revise our manuscript. We highly appreciate the reviewer for their comments and suggestions on the manuscript entitled "**Mechanistic and Kinetics Investigations of Oligomer Formation from Criegee Intermediates Reactions with Hydroxyalkyl Hydroperoxides**". We have made revisions of our manuscript carefully according to the comments and suggestions of reviewer. The revised contents are marked in blue color. The response letter to reviewers is attached at the end of this cover letter.

We hope that the revised manuscript can meet the requirement of Atmospheric Chemistry & Physics. Any further modifications or revisions, please do not hesitate to contact us.

Look forward to hearing from you as soon as possible.

Best regards,

Yu Huang

Comments of reviewer #2

1. First of all, I think that the title of this study goes too far. The main focus of this study refers just to the reaction of Carbonyl oxides with HHPs, although a second step, namely the mechanisms for the interaction of the products of these reaction with Carbonyl oxides is taken into account.

Response: The title of this study has been revised to "Mechanistic and Kinetics Investigations of Oligomer formation from Criegee Intermediates Reactions with Hydroxyalkyl Hydroperoxides".

2. Along the text, the authors refer to several reaction products, as for instance, P2c, P2b and so on, but the structure of these compounds is not mentioned, which makes the work difficult to follow.

Response: Based on the Reviewer's suggestion, the structures of all reactants and products are added in the revised manuscript and supplement figures.

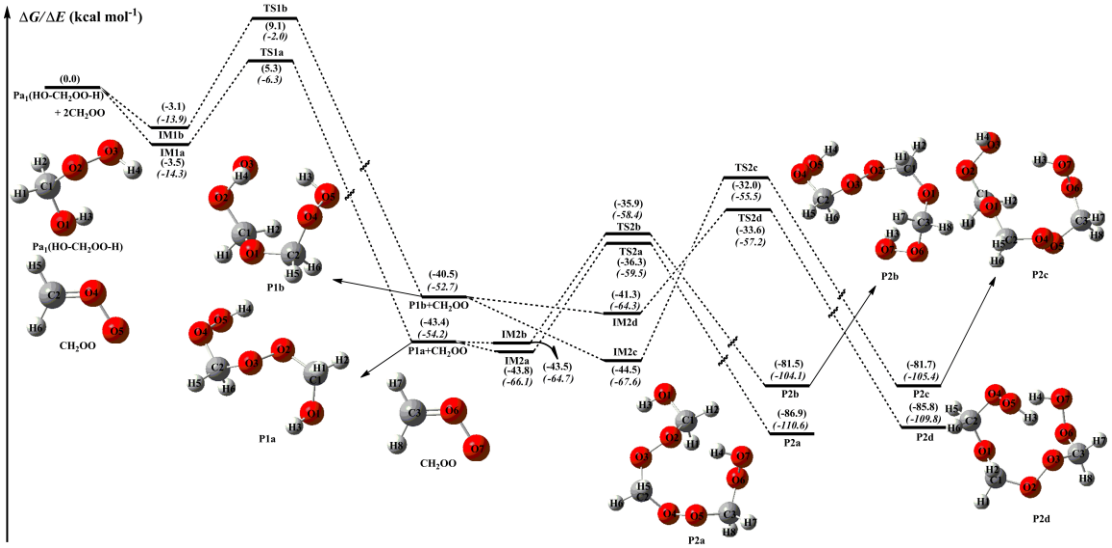

Figure 2. *PES (ΔG and ΔE (italic)) for the reaction of CH_2OO with HO-CH_2OO-H (Pa_1) computed at the M06-2X/def2-TZVP//M06-2X/6-311+G(2df,2p) level of theory*

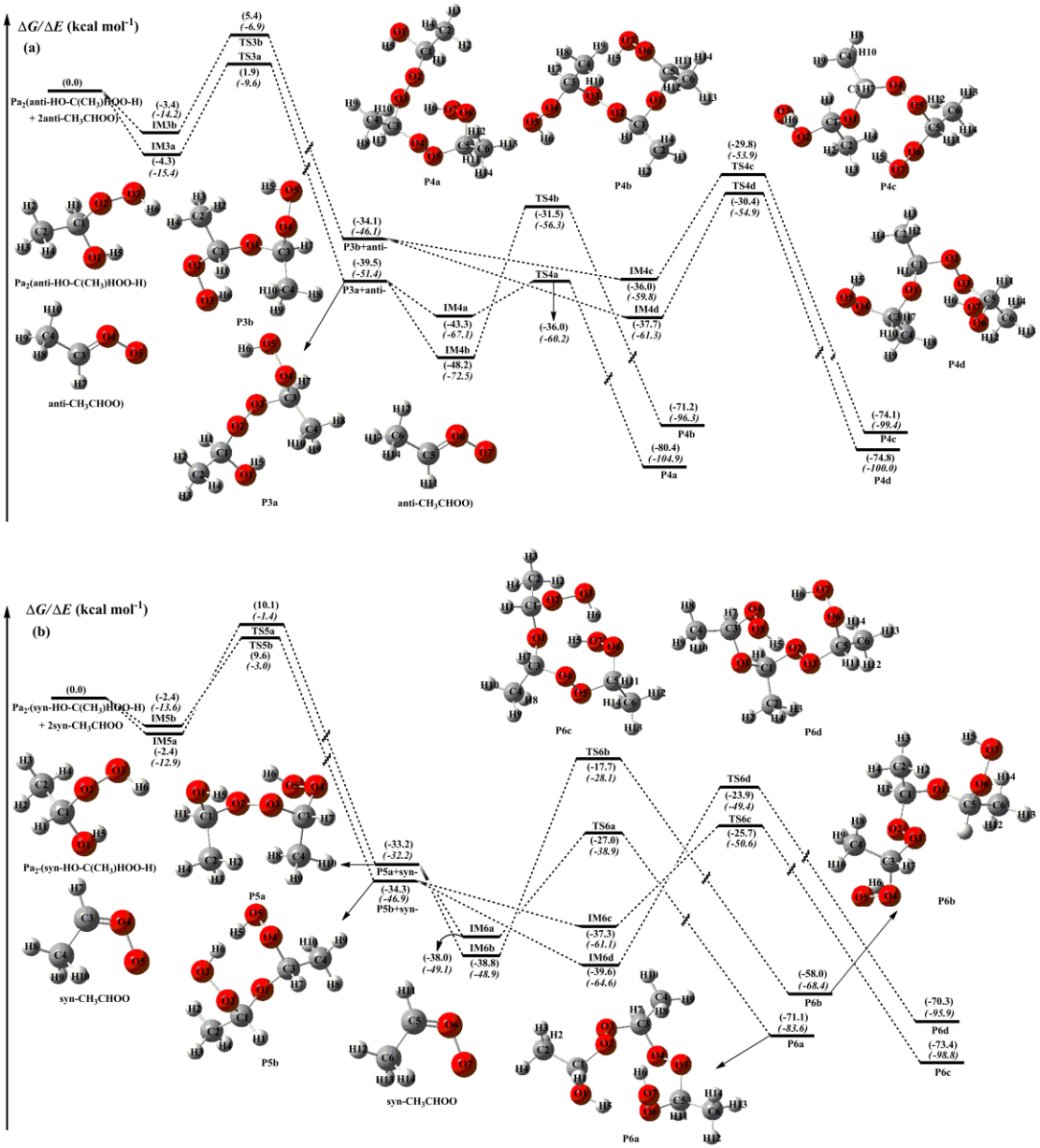

Figure 3. *PES (ΔG and ΔE (italic)) for the reactions of HO-C(CH_3)HOO-H with anti-(a) and syn-CH_3CHOO(b) calculated at the M06-2X/def2-TZVP//M06-2X/6-311+G(2df,2p) level of theory*

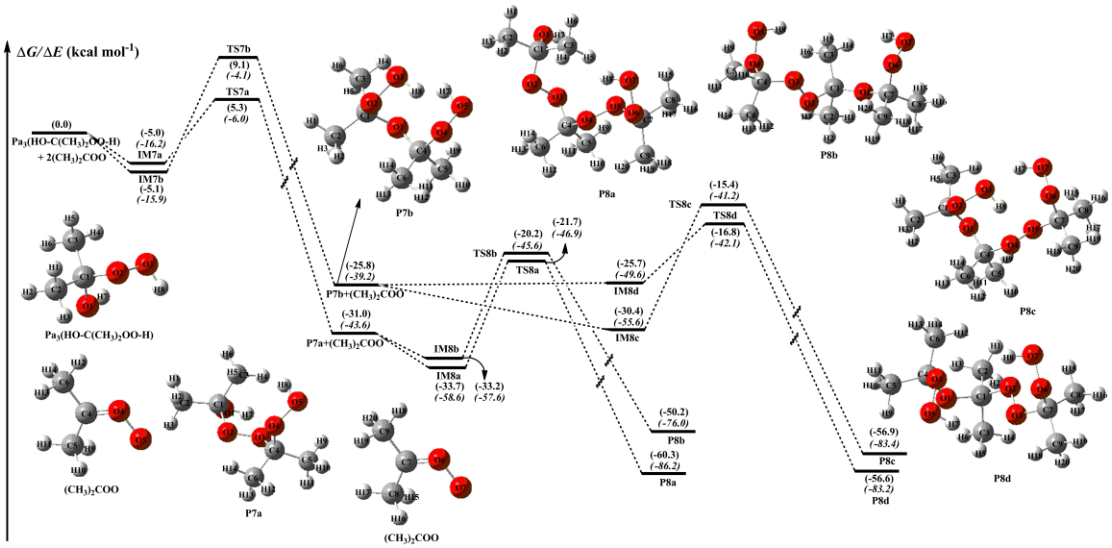

Figure 4. *PES (ΔG and ΔE (italic)) for the reaction of $(CH_3)_2COO$ with HO-C$(CH_3)_2$OO-H(Pa_3) calculated at the M06-2X/def2-TZVP//M06-2X/6-311+G(2df,2p) level of theory*

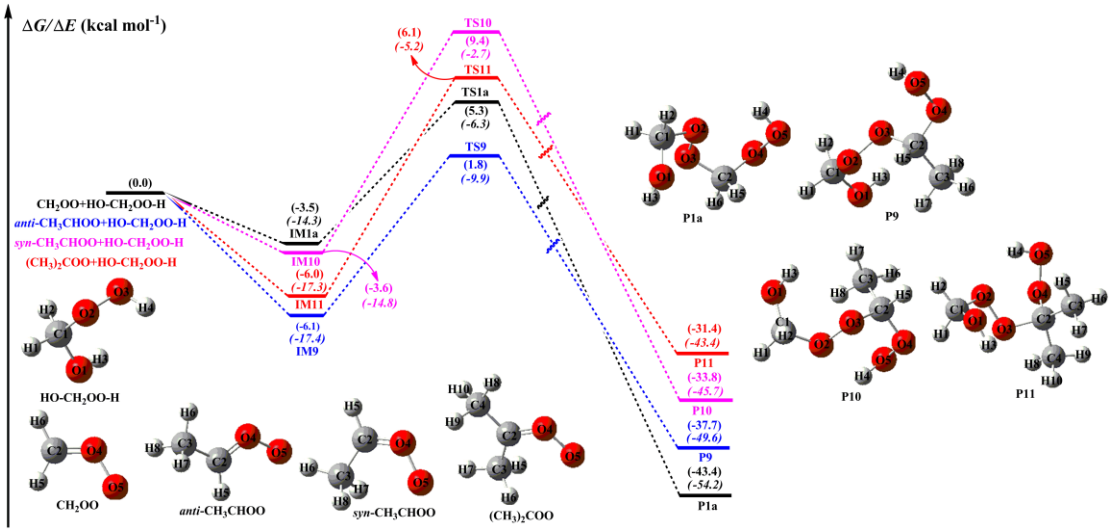

Figure 5. *PES (ΔG and ΔE (italic)) of distinct SCI reactions with HO-CH_2OO-H (Pa_1) calculated at the M06-2X/def2-TZVP//M06-2X/6-311+G(2df,2p) level of theory*

3. Some important references misses, as for instance CPL, 2001,337, 199, JPCA, 2001,105,446, JACS, 1997, 119, 330, CPC 2002, 2, 215, JPCA, 2003, 107, 5812, J. Atmos. Chem, 2000, 35, 165 and references therein.

Response: The references on the unimolecular decay of HHPs generated from isoprene ozonolysis, and OH radicals production from alkene ozonolysis are added in the Introduction of the revised manuscript. Thanks for suggesting these closely related references, which have now been cited in the revised manuscript.

The corresponding sentences have been added in the page 4 line 90-92, page 6 line 145-148 and page 3 line 57-61 of the revised manuscript in blue color:

Winterhalter et al. (2001) studied the mechanism and products of gas phase ozonolysis of β-pinene, and found that the main products are the excited C9-CI plus HCHO. Aplincourt et al. (2003) investigated the unimolecular decay and water-catalyzed decomposition of HHPs generated from isoprene ozonolysis, and found that the main products are methyl vinyl ketone (MVK) or methacroleine (MAC) plus H_2O_2. The thermal unimolecular decay of vibrationally excited CIs is thought to be an important nonphotolytic source of atmospheric hydroxyl (OH) radicals, particularly in low light conditions, urban environments, and heavily forested areas (Lester et al., 2018; Foreman et al., 2016; Kidwell et al., 2016; Green et al., 2017; Zhang et al., 2002; Cremer et al., 2001; Anglada et al., 2002).

4. Regarding the theoretical approach, the authors state that all stationary points have been computing using the M06-2X functional, and for some selected elementary reactions they have performed single point energy calculations at CCSD(T) level of theory, pointing out that the deviations in the free energy barriers computed with both approaches range between 1.5-1.6 kcal/mol. The authors should clarify in which cases they have computed the energy barriers using both approaches, if they have taken into account basis set superposition corrections. They should compare the results of both approaches, for instance with results from the literature involving the reaction with water vapor (section 3.1) with results from the literature, where energy barriers are reported at CCSD(T)/CBS level of theory.

Response: In the present study, the geometries of all stationary points on PES are optimized at the M06-2X/6-311+G(2df,2p) level of theory. For improved energies, single point calculations at the M06-2X/def2-TZVP level are performed. In order to evaluate the reliability of M06-2X functional in computing energies, the single point energies of species involved in the some selected elementary reactions (R1a-R1d, R3a-R3d and R5a-R5d) are recalculated at the CCSD(T)/6-311+G(2df,2p) level based on the M06-2X/6-311+G(2df,2p) optimized geometries. Furthermore, the basis set superposition error (BSSE) is performed using the counterpoise method proposed by Boys and Bernardi (Boys et al., 1970). The electronic-energy ($\Delta E_a^{\#}$) and free-energy ($\Delta G_a^{\#}$) barriers comparisons of both approaches for considering BSSE correction and not considering are listed in Table S1. As shown in Table S1, the BSSE correction contributes to the barriers ~ 1.4 (CCSD(T)) and ~ 0.4 (M06-2X) kcal·mol^{-1}, respectively. The mean absolute deviations (MAD) of both approaches are 0.98 ($\Delta E_a^{\#}$) and 0.96 ($\Delta G_a^{\#}$) kcal·mol^{-1} when without

considering BSSE correction, while they are 0.38 ($\Delta E_a^{\#}$) and 0.34 ($\Delta G_a^{\#}$) kcal mol^{-1} when considering BSSE correction. The result shows that the M06-2X method in combination with the BSSE correction afford energies similar to those determined by the accurate and well recognized CCSD(T) level calculation. Considering the computational costs, the M06-2X/def2-TZVP method is selected to perform the single-point energy calculation for the title reaction system.

For the bimolecular reaction of carbonyl oxide with water dimer, the barriers ($\Delta E_a^{\#}$ and ($\Delta G_a^{\#}$) are calculated using the M06-2X/def2-TZVP//M06-2X/6-311+G(2df,2p) method, and compared to the literature results. As shown in Table 1, the barrier differences between the computational and literature ones that were derived from the CCSD(T)/aug-cc-pVTZ//B3LYP/6-311+G(2df,2p) method (Anglada et al., 2016) are 0.5-1.0 kcal mol^{-1}. Such discrepancies may be attributed to the different theoretical methods used in computing energies. The barrier of Entry 4 is 3.3 kcal mol^{-1}, which is lower than the corresponding CCSD(T)/CBS result by 0.5 kcal mol^{-1} (Anglada et al., 2016). The results show that the M06-2X method provides energies similar to those determined by the CCSD(T) level calculation.

Corresponding descriptions have been added in the page 8 line 198-215 and page 10 line 264-271 of the revised manuscript:

In order to obtain a better evaluation on the reliability of M06-2X functional in computing energies, the single point energies of species included in some selected elementary reactions (R1a-R1d, R3a-R3d and R5a-R5d) are recalculated at the CCSD(T)/6-311+G(2df,2p) level based on the M06-2X/6-311+G(2df,2p) optimized geometries. Furthermore, the basis set superposition error (BSSE) is performed using the counterpoise method described by Boys and Bernardi (1970) to estimate the stability of the pre-reactive complexes. The electronic-energy ($\Delta E_a^{\#}$) and free-energy ($\Delta G_a^{\#}$) barriers comparisons of both approaches for considering BSSE correction and not considering are listed in Table S1. As shown in Table S1, the contributions of BSSE corrections to the barriers are ~ 1.4 (CCSD(T)) and ~ 0.4 (M06-2X) kcal mol^{-1}, respectively. The mean absolute deviations (MAD) of both approaches are 0.98 ($\Delta E_a^{\#}$) and 0.96 ($\Delta G_a^{\#}$) kcal mol^{-1} when without considering BSSE correction, while they become 0.38 ($\Delta E_a^{\#}$) and 0.34 ($\Delta G_a^{\#}$) kcal mol^{-1} when considering BSSE correction. The result shows that the M06-2X method in combination with the BSSE correction afford energies similar to those determined by the accurate and well recognized CCSD(T) level calculation. Considering the computational costs, the

M06-2X/def2-TZVP method is selected to perform the single-point energy calculation for the title reaction system.

As shown in Table 1, the barrier differences between the computational and literature ones that were derived from the CCSD(T)/aug-cc-pVTZ//B3LYP/6-311+G(2df,2p) method (Anglada et al., 2016) are 0.5-1.0 kcal mol^{-1}. Such discrepancies may be attributed to the different theoretical method used in computing energies. The barrier of Entry 4 is 3.3 kcal mol^{-1}, which is lower than the corresponding CCSD(T)/CBS result by 0.5 kcal mol^{-1} (Anglada et al., 2016). The results show that the M06-2X method provides energies similar to those determined by the CCSD(T) level calculation.

Table 1 *Relative free-energies (kcal mol^{-1}) for the stationary points and free-energy ($\Delta G_a^{\#}$) barriers for the elementary pathways of distinct carbonyl oxides reactions with water dimer calculated at the M06-2X/def2-TZVP//M06-2X/6-311+G(2df,2p) level of theory. Labels A, B, C, and D are defined in Figure 1*

Entry	*R1*	*R2*	*DO2H4O4H3*	*DO4H2O3H1*	*A*	*B*	*C*	*D*	$\Delta G_a^{\#}$
1	*H*	*H*	*-123.6*	*96.7*	*-2.5(-2.9)*	*0.2*	*-40.5*	*-39.9*	*2.7 [2.2]*
2	*H*	*H*	*124.5*	*-94.9*	*-2.5(-3.0)*	*0.2*	*-39.6*	*-40.2*	*2.7*
3	*H*	*H*	*-143.8*	*-116.9*	*-2.2(-2.6)*	*0.2*	*-39.1*	*-40.2*	*2.4*
4	*H*	*H*	*143.0*	*122.7*	*-1.9(-2.3)*	*1.4*	*-40.0*	*-40.3*	*3.3 {3.8}*
5	*CH_3*	*H*	*-126.2*	*100.9*	*-2.5(-3.0)*	*4.1*	*-32.4*	*-31.9*	*6.6 [6.0]*
6	*CH_3*	*H*	*130.0*	*-90.4*	*-2.0(-2.5)*	*4.3*	*-31.6*	*-32.2*	*6.3*
7	*CH_3*	*H*	*-146.0*	*-116.3*	*-2.1(-2.6)*	*4.1*	*-30.9*	*-32.2*	*6.2*
8	*CH_3*	*H*	*138.1*	*126.3*	*-2.3(-2.8)*	*4.7*	*-31.7*	*-31.9*	*7.0*
9	*H*	*CH_3*	*-122.1*	*95.0*	*-4.3(-4.8)*	*0.6*	*-36.6*	*-36.2*	*4.9 [3.9]*
10	*H*	*CH_3*	*125.6*	*-93.6*	*-3.9(-4.3)*	*0.7*	*-35.7*	*-36.5*	*4.6*
11	*H*	*CH_3*	*-138.1*	*-120.5*	*-4.4(-4.9)*	*1.1*	*-34.9*	*-36.5*	*5.5*
12	*H*	*CH_3*	*139.2*	*123.4*	*-3.6(-4.1)*	*2.0*	*-36.0*	*-36.2*	*5.6*
13	*CH_3*	*CH_3*	*-125.4*	*101.5*	*-4.6(-5.1)*	*4.2*	*-29.7*	*-29.1*	*8.8 [7.8]*
14	*CH_3*	*CH_3*	*128.5*	*-89.8*	*-4.2(-4.8)*	*4.5*	*-28.6*	*-29.7*	*8.7*
15	*CH_3*	*CH_3*	*-145.4*	*-117.6*	*-4.9(-5.3)*	*4.6*	*-28.2*	*-29.7*	*9.5*
16	*CH_3*	*CH_3*	*136.3*	*129.4*	*-4.5(-5.0)*	*5.2*	*-29.2*	*-29.1*	*9.7*

Values in parenthesis correspond to without considering the BSSE correction, values in brackets correspond to CCSD(T)/aug-cc-pVTZ//B3LYP/6-311+G(2df,2p), values in braces correspond to CCSD(T)/CBS//B3LYP/6-311+G(2df,2p)

Table S1 *Y/X (Y = M06-2X, CCSD(T), X = 6-311+G(2df,2p), def2-TZVP) calculated energy*

barrier($\Delta E_a^{\#}$, $\Delta G_a^{\#}$) for the addition reactions of carbonyl oxides with HHPs based on the M06-2X/6-311+G(2df,2p) optimized geometries (kcal mol^{-1})

Reactions	CCSD(T)/6-311+G(2df,2p)		M06-2X/def2-TZVP	
	$\Delta E_a^{\#}$	$\Delta G_a^{\#}$	$\Delta E_a^{\#}$	$\Delta G_a^{\#}$
R1a	9.4[a]; 7.9[b]	10.1[a]; 8.6[b]	8.0[a]; 7.6[b]	8.8[a]; 8.4[b]
R1b	13.0[a]; 11.6[b]	13.3[a]; 11.9[b]	11.9[a]; 11.4[b]	12.2[a]; 11.7[b]
R1c	8.1[a]; 6.7[b]	9.2[a]; 7.8[b]	6.9[a]; 6.4[b]	7.9[a]; 7.4[b]
R1d	8.6[a]; 7.6[b]	10.2[a]; 9.2[b]	7.0[a]; 6.7[b]	8.7[a]; 8.4[b]
R3a	6.6[a]; 4.9[b]	7.1[a]; 5.4[b]	5.8[a]; 4.4[b]	6.2[a]; 5.8[b]
R3b	8.4[a]; 7.3[b]	9.7[a]; 8.6[b]	7.3[a]; 6.8[b]	8.8[a]; 8.3[b]
R3c	6.5[a]; 4.8[b]	7.3[a]; 5.6[b]	5.8[a]; 5.4[b]	6.6[a]; 6.2[b]
R3d	8.4[a]; 6.8[b]	9.7[a]; 8.1[b]	7.3[a]; 6.8[b]	8.6[a]; 8.1[b]
R5a	12.3[a]; 10.9[b]	13.2[a]; 11.8[b]	11.5[a]; 11.1[b]	12.5[a]; 12.1[b]
R5b	11.0[a]; 9.4[b]	12.4[a]; 10.8[b]	10.6[a]; 10.1[b]	12.0[a]; 11.5[b]
R5c	12.0[a]; 10.6[b]	13.3[a]; 11.9[b]	11.3[a]; 10.9[b]	12.5[a]; 12.1[b]
R5d	12.2[a]; 11.0[b]	13.8[a]; 12.6[b]	11.4[a]; 11.0[b]	13.0[a]; 12.6[b]

a and b represent without and with considering the BSSE correction

5. Regarding the kinetics, the authors should clarify if they have considered the pre-reactive complexes in the kinetic study and if they play a role in the temperature dependence of the rate constants.

Response: As shown in Figure 5, the CH_2OO + HO-CH_2OO-H (Pa_1) reaction proceeds according to a two-step mechanism: (i) a fast thermal equilibrium between the reactants and intermediate IM1a, (ii) the addition of CH_2OO leading to the formation of product P1a. The whole reaction process is expressed as follows:

$$CH_2OO + HO\text{-}CH_2OO\text{-}H \underset{k_{-1}}{\overset{k_1}{\rightleftharpoons}} IM1a \xrightarrow{k_2} TS1a \rightarrow P1a \quad (5)$$

Applying the steady state approximation (SSA) for the intermediate IM1a, the overall rate coefficient is extrapolated to the eqn (6): (Zhang et al., 2012; Liu et al., 2015)

$$k_{ovr} = \frac{k_1 \times k_2}{k_{-1} + k_2} \quad (6)$$

If $k_2 << k_{-1}$, the overall rate coefficient is written as follows: (Ryzhkov et al., 2006; Chen et al., 2016)

$$k_{ovr} = \frac{k_1 \times k_2}{k_{-1} + k_2} \approx \frac{k_1}{k_{-1}} k_2 = K_{eq} k_2 \quad (7)$$

The equilibrium coefficient K_{eq} is expressed as eqn (8):

$$K_{eq} = \sigma \frac{Q_{IM}(T)}{Q_A(T)Q_B(T)} \exp\left(\frac{G_R - G_{IM}}{RT}\right) \quad (8)$$

where σ is reaction symmetry number, $Q_{IM}(T)$, $Q_A(T)$ and $Q_B(T)$ denote the products of electronic, translational, rotational, torsional, and vibrational canonical partition functions for the intermediate, reactants A and B, respectively (Mendes, et al., 2014), T is the temperature in Kelvin, G_R and G_{IM} are the total free-energies of the reactant and intermediate, respectively.

Table R1 lists the partition functions, equilibrium coefficients (K_{eq}), and rate coefficients ($k_{2(IM1a-TS1a)}$ and $k_{ovr(R1a)}$) of the bimolecular reaction of CH_2OO with HO-CH_2OO-H (Pa_1). As shown the Table R1, the partition functions of reactants and intermediate increase with raising temperature, whereas the $k_{ovr(R1a)}$, K_{eq} and $k_{2(IM1a-TS1a)}$ decrease with increasing temperature, indicating that there is not a direct correlation between $k_{ovr(R1a)}$ and partition function of pre-reactive intermediate. The result shows that the kinetics parameters strongly depend on the interaction between K_{eq} and $k_{2(IM1a-TS1a)}$. Similar conclusions are also obtained from those of the *anti*-CH_3CHOO + HO-CH_2OO-H(R9), *syn*-CH_3CHOO + HO-CH_2OO-H(R10) and $(CH_3)_2CHOO$ + HO-CH_2OO-H(R11) systems (Table R2-R4).

Table R1 The partition function, equilibrium coefficient (K_{eq}) (cm^3 $molecule^{-1}$), and rate coefficients ($k_{2(IM1a-TS1a)}$ and $k_{ovr(R1a)}$) (cm^3 $molecule^{-1}$ s^{-1}) of CH_2OO reactions with HO-CH_2OO-H (Pa_1) computed at different temperatures

T/K	Q_{CH2OO}	$Q_{HOCH2OOH}$	Q_{IMa}	K_{eq}	$k_{2(IM1a-TS1a)}$	$k_{ovr(R1a)}$
273	7.9×10^{10}	1.6×10^{12}	1.1×10^{15}	2.8×10^{-6}	4.3×10^{-6}	1.2×10^{-11}
280	8.8×10^{10}	1.9×10^{12}	1.5×10^{15}	2.4×10^{-6}	4.0×10^{-6}	9.4×10^{-12}
298	1.2×10^{11}	2.7×10^{12}	2.7×10^{15}	$1.6 \times 10\text{-}^{6}$	3.3×10^{-6}	5.4×10^{-12}
300	1.2×10^{11}	2.8×10^{12}	2.9×10^{15}	1.6×10^{-6}	3.2×10^{-6}	5.1×10^{-12}
320	1.6×10^{11}	4.2×10^{12}	5.6×10^{15}	1.1×10^{-6}	2.7×10^{-6}	3.0×10^{-12}
340	2.1×10^{11}	6.2×10^{12}	1.1×10^{16}	8.1×10^{-7}	2.3×10^{-6}	1.9×10^{-12}
360	2.7×10^{11}	9.0×10^{12}	2.0×10^{16}	6.2×10^{-7}	2.0×10^{-6}	1.2×10^{-12}
380	3.5×10^{11}	1.3×10^{13}	3.6×10^{16}	4.8×10^{-7}	1.8×10^{-6}	8.6×10^{-13}
400	4.5×10^{11}	1.8×10^{13}	6.6×10^{16}	3.9×10^{-7}	1.6×10^{-6}	6.3×10^{-13}

Table R2 The partition function, equilibrium coefficient (K_{eq}) (cm^3 $molecule^{-1}$), and rate coefficients ($k_{2(IM9-TS9)}$ and $k_{ovr(R9)}$) (cm^3 $molecule^{-1}$ s^{-1}) of *anti*-CH_3CHOO reactions with HO-CH_2OO-H (Pa_1) computed at different temperatures

T/K	$Q_{anti-CH3CHOO}$	$Q_{HOCH2OOH}$	Q_{IM9}	K_{eq}	$k_{2(IM9-TS9)}$	$k_{ovr(R9)}$
273	1.4×10^{12}	1.6×10^{12}	9.1×10^{15}	1.3×10^{-4}	4.4×10^{-5}	5.5×10^{-9}
280	1.6×10^{12}	1.9×10^{12}	1.2×10^{16}	9.6×10^{-5}	3.9×10^{-5}	3.7×10^{-9}
298	2.4×10^{12}	2.7×10^{12}	2.5×10^{16}	5.0×10^{-5}	2.9×10^{-5}	1.5×10^{-9}

300	2.5×10^{12}	2.8×10^{12}	2.7×10^{16}	4.7×10^{-5}	2.9×10^{-5}	1.3×10^{-9}
320	3.7×10^{12}	4.2×10^{12}	5.8×10^{16}	2.5×10^{-5}	2.2×10^{-5}	5.5×10^{-10}
340	5.4×10^{12}	6.2×10^{12}	1.2×10^{17}	1.5×10^{-5}	1.7×10^{-5}	2.6×10^{-10}
360	7.8×10^{12}	9.0×10^{12}	2.5×10^{17}	9.1×10^{-6}	1.4×10^{-5}	1.3×10^{-10}
380	1.1×10^{13}	1.3×10^{13}	5.1×10^{17}	5.9×10^{-6}	1.2×10^{-5}	7.1×10^{-11}
400	1.6×10^{13}	1.8×10^{13}	1.0×10^{18}	4.1×10^{-6}	1.0×10^{-5}	4.1×10^{-11}

Table R3 The partition function, equilibrium coefficient (K_{eq}) (cm^3 $molecule^{-1}$), and rate coefficients ($k_{2(IM10-TS10)}$ and $k_{ovr(R10)}$) (cm^3 $molecule^{-1}$ s^{-1}) of *syn*-CH_3CHOO reactions with HO-CH_2OO-H (Pa_1) computed at different temperatures

T/K	$Q_{syn\text{-}CH3CHOO}$	$Q_{HOCH2OOH}$	Q_{IM10}	K_{eq}	$k_{2(IM10-TS10)}$	$k_{ovr(R10)}$
273	1.0×10^{12}	1.6×10^{12}	6.6×10^{15}	1.5×10^{-6}	5.6×10^{-9}	8.1×10^{-15}
280	1.2×10^{12}	1.9×10^{12}	8.8×10^{15}	1.2×10^{-6}	6.0×10^{-9}	7.5×10^{-15}
298	1.7×10^{12}	2.7×10^{12}	1.8×10^{16}	8.6×10^{-7}	7.3×10^{-9}	6.3×10^{-15}
300	1.8×10^{12}	2.8×10^{12}	1.9×10^{16}	8.3×10^{-7}	7.5×10^{-9}	6.2×10^{-15}
320	2.6×10^{12}	4.2×10^{12}	4.1×10^{16}	5.8×10^{-7}	9.1×10^{-9}	5.3×10^{-15}
340	3.7×10^{12}	6.2×10^{12}	8.7×10^{16}	4.3×10^{-7}	1.1×10^{-8}	4.6×10^{-15}
360	5.3×10^{12}	9.0×10^{12}	1.8×10^{17}	3.3×10^{-7}	1.3×10^{-8}	4.1×10^{-15}
380	7.5×10^{12}	1.3×10^{13}	3.6×10^{17}	2.6×10^{-7}	1.5×10^{-8}	3.8×10^{-15}
400	1.1×10^{13}	1.8×10^{13}	7.2×10^{17}	2.1×10^{-7}	1.7×10^{-8}	3.5×10^{-15}

Table R4 The partition function, equilibrium coefficient (K_{eq}) (cm^3 $molecule^{-1}$), and rate coefficients ($k_{2(IM11-TS11)}$ and $k_{ovr(R11)}$) (cm^3 $molecule^{-1}$ s^{-1}) of $(CH_3)_2CHOO$ reactions with HO-CH_2OO-H (Pa_1) computed at different temperatures

T/K	$Q_{(CH3)2CHOO}$	$Q_{HOCH2OOH}$	Q_{IM11}	K_{eq}	$k_{2(IM10-TS10)}$	$k_{ovr(R10)}$
273	7.2×10^{12}	1.6×10^{12}	4.0×10^{16}	8.8×10^{-5}	3.1×10^{-8}	2.7×10^{-12}
280	8.5×10^{12}	1.9×10^{12}	5.5×10^{16}	6.9×10^{-5}	3.4×10^{-8}	2.3×10^{-12}
298	1.3×10^{13}	2.7×10^{12}	1.2×10^{17}	3.7×10^{-5}	4.1×10^{-8}	1.5×10^{-12}
300	1.4×10^{13}	2.8×10^{12}	1.3×10^{17}	3.5×10^{-5}	4.2×10^{-8}	1.5×10^{-12}
320	2.2×10^{13}	4.2×10^{12}	3.2×10^{17}	1.9×10^{-5}	5.2×10^{-8}	1.0×10^{-12}
340	3.5×10^{13}	6.2×10^{12}	7.3×10^{17}	1.2×10^{-5}	6.2×10^{-8}	7.2×10^{-13}
360	5.5×10^{13}	9.0×10^{12}	1.7×10^{18}	7.4×10^{-6}	7.4×10^{-8}	5.4×10^{-13}
380	8.6×10^{13}	1.3×10^{13}	3.8×10^{18}	5.0×10^{-6}	8.6×10^{-8}	4.2×10^{-13}
400	1.3×10^{14}	1.8×10^{13}	8.3×10^{18}	3.5×10^{-6}	9.8×10^{-8}	3.4×10^{-13}

The corresponding sentences have been added in the page 9 line 219-237 of the revised manuscript in blue color:

As shown in Figure 5, the CH_2OO + HO-CH_2OO-H (Pa_1) reaction proceeds according to a two-step mechanism: (i) a fast thermal equilibrium between the reactants and intermediate IM1a, (ii) the addition of CH_2OO leading to the formation of product P1a. The whole reaction process is expressed as follows:

$$CH_2OO + HO\text{-}CH_2OO\text{-}H \underset{k_{-1}}{\overset{k_1}{\rightleftarrows}} IM1a \xrightarrow{k_2} TS1a \rightarrow P1a \quad (4)$$

Applying the steady state approximation (SSA) for the intermediate IM1a, the overall rate coefficient is extrapolated to the eqn (5) (Zhang et al., 2012; Liu et al., 2015)

$$k_{ovr} = \frac{k_1 \times k_2}{k_{-1} + k_2} \quad (5)$$

If $k_2 << k_{-1}$, the overall rate coefficient is written as follows: (Chen et al., 2016b; Ryzhkov et al., 2006)

$$k_{ovr} = \frac{k_1 \times k_2}{k_{-1} + k_2} \approx \frac{k_1}{k_{-1}} k_2 = K_{eq} k_2 \quad (6)$$

The equilibrium coefficient K_{eq} is expressed as eqn (7):

$$K_{eq} = \sigma \frac{Q_{IM}(T)}{Q_A(T) Q_B(T)} \exp\left(\frac{G_R - G_{IM}}{RT}\right) \quad (7)$$

where σ is reaction symmetry number, $Q_{IM}(T)$, $Q_A(T)$ and $Q_B(T)$ denote the products of electronic, translational, rotational, torsional, and vibrational canonical partition functions for the intermediate, reactants A and B, respectively (Mendes et al., 2014), T is the temperature in Kelvin, G_R and G_{IM} are the total free-energies of the reactant and complex, respectively.

6. The authors report rate constants for the reactions of the carbonyl oxides considered with HHP's (Table 2), but no mention is done for the reactions of P1x with Carbonyl oxides. Moreover, that authors should clarify if they have considered all different conformers of the stationary points in the kinetic study. In addition, they should estimate the errors in the these calculated rate constants, since they can be between one and two orders of magnitude according to the errors in the computed free energy barriers.

Response: Based on the Reviewer's suggestion, the rate coefficients of carbonyl oxides reactions with P1x, P3x, P5x, and P7x are calculated using a combination of canonical transition state theory (CTST) and an asymmetric Eckart tunneling correction at 273-400 K. And the different conformers of stationary points in the kinetics study are taken into account, with the obtained results listed in Table S5-S8. As shown in Table S5, the predicted rate coefficients for the reaction of CH_2OO with P1a decrease with increasing temperature, with a similar trend observed for CH_2OO + P1b, CH_2OO + P1c and CH_2OO + P1d systems. The result implies that the oligomer

formation from CH_2OO reaction with HHP is preferable under low temperature conditions. Similar conclusions are obtained from the *anti*-CH_3CHOO + P3x (Table S6), *syn*-CH_3CHOO + P5x (Table S7) and $(CH_3)_2CHOO$ + P7x (Table S8) systems. In order to avoid redundancy, we do not repeat them here in detail. Considering the errors of the computed free energy barriers, the uncertainty of rate coefficient is estimated within an order of magnitude.

Corresponding descriptions have been added in the page 18 line 500-506 and page 19 line 521-528 of the revised manuscript:

the rate coefficients of distinct SCI reactions with HO-CH_2OO-H (Pa_1) are computed using a combination of canonical transition state theory (CTST) and an asymmetric Eckart tunneling correction based on the free energies obtained at the M06-2X level, in the temperature range from 273 to 400 K. And the different conformers of stationary points in the kinetics study are taken into account, with the results listed in Table 2 and Table S5-S8.

As shown in Table S5, the rate coefficients of CH_2OO + P1a, CH_2OO + P1b, CH_2OO + P1c and CH_2OO + P1d reactions decrease with increasing temperature, indicating that the oligomer formation from CH_2OO reactions with HHP is preferable under low temperature conditions. Similar conclusions are also obtained from the anti-CH_3CHOO + P3x (Table S6), syn-CH_3CHOO + P5x (Table S7) and $(CH_3)_2CHOO$ + P7x (Table S8) systems. In order to avoid redundancy, we do not repeat them here in detail. Considering the errors of the computed free energy barriers, the uncertainty of rate coefficient is estimated within an order of magnitude.

Table S5 *Rate coefficients (cm^3 $molecule^{-1}$ s^{-1}) of CH_2OO reactions with P1a, P1b, P1c and P1d computed at different temperatures*

T/K	$k_{(CH2OO+P1a)}$	$k_{(CH2OO+P1b)}$	$k_{(CH2OO+P1c)}$	$k_{(CH2OO+P1d)}$
273	5.1×10^{-12}	3.5×10^{-12}	8.2×10^{-13}	4.8×10^{-11}
280	4.0×10^{-12}	2.9×10^{-12}	7.1×10^{-13}	3.7×10^{-11}
298	2.3×10^{-12}	1.9×10^{-12}	5.2×10^{-13}	1.9×10^{-11}
300	2.2×10^{-12}	1.8×10^{-12}	5.0×10^{-13}	1.8×10^{-11}
320	1.3×10^{-12}	1.2×10^{-12}	3.7×10^{-13}	1.0×10^{-11}
340	8.3×10^{-13}	8.5×10^{-13}	2.8×10^{-13}	5.9×10^{-12}
360	5.6×10^{-13}	6.3×10^{-13}	2.3×10^{-13}	3.8×10^{-12}
380	4.0×10^{-13}	4.9×10^{-13}	1.9×10^{-13}	2.5×10^{-12}
400	3.0×10^{-13}	3.9×10^{-13}	1.6×10^{-13}	1.8×10^{-12}

Table S6 *Rate coefficients (cm^3 $molecule^{-1}$ s^{-1}) of anti-CH_3CHOO reactions with P3a, P3b, P3c and P3d computed at different temperatures*

T/K	$k_{(anti+P3a)}$	$k_{(anti+P3b)}$	$k_{(anti+P3c)}$	$k_{(anti+P3d)}$
273	3.5×10^{-9}	2.3×10^{-9}	1.7×10^{-7}	2.1×10^{-9}
280	2.3×10^{-9}	1.4×10^{-9}	1.0×10^{-7}	1.4×10^{-9}
298	8.8×10^{-10}	5.8×10^{-10}	2.9×10^{-8}	5.9×10^{-10}
300	8.0×10^{-10}	5.3×10^{-10}	2.6×10^{-8}	5.4×10^{-10}
320	3.2×10^{-10}	2.3×10^{-10}	7.9×10^{-9}	2.3×10^{-10}
340	1.4×10^{-10}	1.1×10^{-10}	2.8×10^{-9}	1.1×10^{-10}
360	7.1×10^{-11}	5.8×10^{-11}	1.1×10^{-9}	5.9×10^{-11}
380	3.8×10^{-11}	3.3×10^{-11}	4.9×10^{-10}	3.4×10^{-11}
400	2.2×10^{-11}	2.0×10^{-11}	2.4×10^{-10}	2.0×10^{-11}

Table S7 *Rate coefficients (cm^3 $molecule^{-1}$ s^{-1}) of syn-CH_3CHOO reactions with P5a, P5b, P5c and P5d computed at different temperatures*

T/K	$k_{(syn+P5a)}$	$k_{(syn+P5b)}$	$k_{(syn+P5c)}$	$k_{(syn+P5d)}$
273	2.1×10^{-11}	1.7×10^{-13}	2.1×10^{-11}	2.4×10^{-13}
280	1.5×10^{-11}	1.4×10^{-13}	1.5×10^{-11}	2.0×10^{-13}
298	7.5×10^{-12}	1.0×10^{-13}	7.6×10^{-12}	1.4×10^{-13}
300	6.9×10^{-12}	9.7×10^{-14}	7.0×10^{-12}	1.4×10^{-13}
320	3.5×10^{-12}	6.9×10^{-14}	3.6×10^{-12}	9.6×10^{-14}
340	1.9×10^{-12}	5.2×10^{-14}	2.0×10^{-12}	7.1×10^{-14}
360	1.1×10^{-12}	4.0×10^{-14}	1.2×10^{-12}	5.5×10^{-14}
380	7.1×10^{-13}	3.0×10^{-14}	7.3×10^{-13}	4.4×10^{-14}
400	4.7×10^{-13}	2.6×10^{-14}	4.9×10^{-13}	3.6×10^{-14}

Table S8 *Rate coefficients (cm^3 $molecule^{-1}$ s^{-1}) of $(CH_3)_2CHOO$ reactions with P7a, P7b, P7c and P7d computed at different temperatures*

T/K	$k_{((CH3)2CHOO+P7a)}$	$k_{((CH3)2CHOO+P7b)}$	$k_{((CH3)2CHOO+P7c)}$	$k_{((CH3)2CHOO+P7d)}$
273	7.8×10^{-14}	9.1×10^{-14}	1.8×10^{-12}	4.5×10^{-13}
280	6.8×10^{-14}	8.2×10^{-14}	1.5×10^{-12}	3.9×10^{-13}
298	5.0×10^{-14}	6.6×10^{-14}	1.0×10^{-12}	2.8×10^{-13}
300	4.8×10^{-14}	6.5×10^{-14}	9.9×10^{-13}	2.7×10^{-13}
320	3.6×10^{-14}	5.3×10^{-14}	6.9×10^{-13}	1.9×10^{-13}
340	2.8×10^{-14}	4.5×10^{-14}	5.1×10^{-13}	1.5×10^{-13}
360	2.2×10^{-14}	3.9×10^{-14}	3.9×10^{-13}	1.2×10^{-13}

380	*1.9 × 10^{-14}*	*3.5 × 10^{-14}*	*3.1 × 10^{-13}*	*9.6 × 10^{-14}*
400	*1.6 × 10^{-14}*	*3.1 × 10^{-14}*	*2.5 × 10^{-13}*	*8.0 × 10^{-14}*

7. With respect to the atmospheric implications, the authors compare the reaction rates of the reaction investigated with those between carbonyl oxides with formic acid. In my opinion, the reactions rates of carbonyl oxides with water and water dimer, but also the reactions rates of HHPs with water should be also taken into account, because the high concentration of water vapor in the atmosphere. For the last, there are free energy barriers in the literature to compare with.

Response: As shown in Table 2, the rate coefficient of *anti*-CH_3CHOO + Pa_1 reaction (R9) is significantly higher than that of the other three pathways (R1a, R10 and R11). Therefore, it would be interesting to investigate whether the *anti*-CH_3CHOO + Pa_1 reaction can compete well with the *anti*-CH_3CHOO + $(H_2O)_2$ (R12) system because the latter reaction is the dominant chemical sink (Anglada et al., 2016; Taatjes, et al., 2013). The ratio of reaction rates of R9 and R12 is expressed as follows

$$\frac{\upsilon_{R9}}{\upsilon_{R12}} = \frac{k_{R9}[CI][Pa_1]}{k_{R12}[CI][(H_2O)_2]} = \frac{k_{R9}[Pa_1]}{k_{R12}[(H_2O)_2]} \quad (9)$$

The room temperature rate coefficient k_{R9} is 1.5 × 10^{-9} cm^3 $molecule^{-1}$ s^{-1}. Assuming that the concentration of Pa_1 is approximately equal to that of SCIs (~ 5.0 × 10^4 molecules cm^{-3}, within an order of magnitude uncertainty) in the boreal forest and rural environments of Finland and Germany (Novelli et al, 2016, 2017). The atmospheric lifetime of *anti*-CH_3CHOO reactivity toward Pa_1 can be estimated as 1.3-13 × 10^3 s. The experimental rate coefficient of reaction R12 approximately equals ~ 1.0 × 10^{-11} cm^3 $molecule^{-1}$ s^{-1} at 298 K (Lin et al., 2016). The concentration of water dimer is 5.5 × 10^{13} molecules cm^{-3} at 3 km altitude (Long et al., 2016). The v_{R9}/v_{R12} ratio is less than 1.4%, meaning that the *anti*-CH_3CHOO + Pa_1 reaction is minor loss process in the atmosphere. However, the $[(H_2O)_2]$ is very low at the altitude above 15 km (< 2.7 × 10^6 molecules cm^{-3}) (Long et al., 2016), the *anti*-CH_3CHOO + Pa_1 reaction can compete well with the *anti*-CH_3CHOO + $(H_2O)_2$ reaction, and thus contribute to the formation and growth of SOA. `

Kumar et al. (2014) proposed that the gas-phase decomposition of Pa_1 has two competitive pathways, namely (i) HO-CH_2OO-H → CH_2O + H_2O_2 and (ii) HO-CH_2OO-H → HCOOH + H_2O. The free energy barriers $\Delta G_a^{\#}$ in the presence of a single water molecule are 31.2 and 47.8 kcal mol^{-1}, respectively, which are 13.5 and 10.2 kcal mol^{-1} lower than the uncatalyzed reactions.

The result reveals that the formaldehyde-forming channel is preferable in the absence and presence of water molecule, and the role of water catalysis on the gas-phase Pa_1 decomposition is significant. The $\Delta G_a^{\#}$ of bimolecular reaction of *anti*-CH_3CHOO with Pa_1 is 7.3 kcal mol^{-1}, which is 23.9 kcal mol^{-1} lower than the formaldehyde-forming channel. It is concluded that the Pa_1 + H_2O reaction is less competitive as compared to the *anti*-CH_3CHOO + Pa_1 system.

Corresponding descriptions have been added in the page 20 line 542-556, page 20 line 565 and page 21 line 566-579 of the revised manuscript:

As discussed above, the anti-CH_3CHOO + HO-CH_2OO-H (Pa_1) reaction (R9) is preferred over the other three pathways (R1a, R10 and R11). Therefore, it would be interesting to investigate whether the anti-CH_3CHOO + Pa_1 reaction can compete well with the anti-CH_3CHOO + $(H_2O)_2$ (R12) system because the latter reaction is the dominant chemical sink (Taatjes et al., 2013; Anglada et al., 2016). The ratio of reaction rates of R9 and R12 is expressed as follows

$$\frac{\upsilon_{R9}}{\upsilon_{R12}} = \frac{k_{R9}[CI][Pa_1]}{k_{R12}[CI][(H_2O)_2]} = \frac{k_{R9}[Pa_1]}{k_{R12}[(H_2O)_2]} \quad (10)$$

The room temperature rate coefficient k_{R9} is 1.5 × 10^{-9} cm^3 $molecule^{-1}$ s^{-1}. Assuming that the concentration of Pa_1 is approximately equal to that of SCIs (~5.0 × 10^4 molecules cm^{-3}, within an order of magnitude uncertainty) in the boreal forest and rural environments of Finland and Germany (Novelli et al., 2016; 2017). The atmospheric lifetime of anti-CH_3CHOO reactivity toward Pa_1 can be estimated as 1.3-13 × 10^3 s. The experimental rate coefficient of reaction R12 approximately equals ~ 1.0 × 10^{-11} cm^3 $molecule^{-1}$ s^{-1} at 298 K (Lin et al., 2016). The concentration of water dimer is 5.5 × 10^{13} molecules cm^{-3} at 3 km altitude (Long et al., 2016).

The v_{R9}/v_{R12} ratio is less than 1.4% when the $[(H_2O)_2]$ is ~ 10^{13} molecules cm^{-3}, meaning that the anti-CH_3CHOO + Pa_1 reaction is minor loss process in the atmosphere. However, the $[(H_2O)_2]$ is very low at the altitude above 15 km, the anti-CH_3CHOO + Pa_1 reaction can compete well with the anti-CH_3CHOO + $(H_2O)_2$ reaction, and thus contribute to the formation and growth of SOA. Kumar et al. (2014) proposed that the gas-phase decomposition of Pa_1 has two competitive pathways: (i) HO-CH_2OO-H → CH_2O + H_2O_2 and (ii) HO-CH_2OO-H → HCOOH + H_2O. The $\Delta G_a^{\#}$ in the presence of a single water molecular are 31.2 and 47.8 kcal mol^{-1}, respectively, which are 13.5 and 10.2 kcal mol^{-1} lower than the uncatalyzed reactions. The result reveals that the formaldehyde-forming channel is preferable in the absence and presence of water molecule, and

the role of water catalysis on the gas-phase decomposition of Pa_1 is significant. The $\Delta G_a^{\#}$ of bimolecular reaction of anti-CH_3CHOO with Pa_1 is 7.3 kcal mol^{-1}, which is 23.9 kcal mol^{-1} lower than the formaldehyde-forming channel. It is concluded that the Pa_1 + H_2O reaction is less competitive as compared to the anti-CH_3CHOO + Pa_1 system.

8. An hydrogen misses in the structure of P1a in Figure 2. In addition some addition structures of the P2x compounds should be drawn if the different figures and the numbers should have a larger size.

Response: Based on the Reviewer's suggestion, the PES of CH_2OO reaction with HO-CH_2OO-H (Pa_1) is redrawn in Figure 2, and the str in the Figure 2.

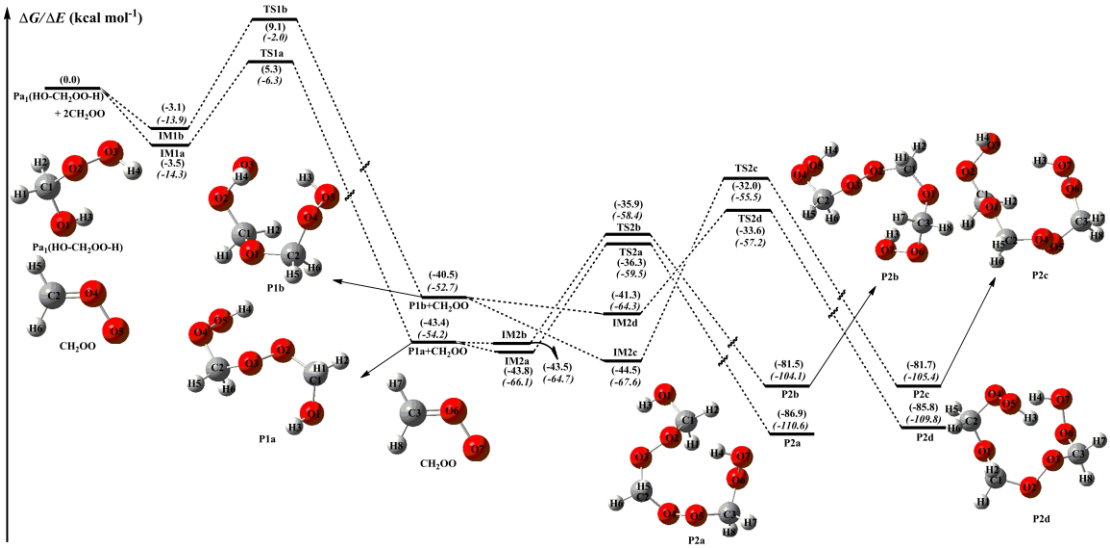

Figure 2. *PES (ΔG and ΔE (italic)) for the reaction of CH_2OO with HO-CH_2OO-H (Pa_1) computed at the M06-2X/def2-TZVP//M06-2X/6-311+G(2df,2p) level of theory*

References

Anglada, J. M., and Solé, A.: Impact of water dimer on the atmospheric reactivity of carbonyl oxides, Phys. Chem. Chem. Phys., 18, 17698-17712, 10.1039/c6cp02531e, 2016.

Boys, S. F., and Bernardi, F.: The calculation of small molecular interactions by the differences of separate total energies. Some procedures with reduced errors, Mol. Phys., 19, 553-566, 10.1080/00268977000101561, 1970.

Chen, L., Wang. W. L., Zhou, L. T., Wang, W. N., Liu, F. Y., Li, C. Y., and Lü, J.: Role of water clusters in the reaction of the simplest Criegee intermediate CH_2OO with water vapour, Theor. Chem. Acc., 135, 252-263, 10.1007/s00214-016-1998-2, 2016.

Kumar, M., Busch, D. H., Subramaniam, B., and Thompson, W. H.: Role of tunable acid catalysis in decomposition of α-hydroxyalkyl hydroperoxides and mechanistic implications for tropospheric chemistry, J. Phys. Chem. A, 118, 9701-9711, 10.1021/jp505100x, 2014.

Lin, L. C., Chang, H. T., Chang, C. H., Chao, W., Smith, M. C., Chang, C. H., Lin, J. J. M., and Takahashi, K.: Competition between H_2O and $(H_2O)_2$ reactions with CH_2OO/CH_3CHOO, Phys. Chem. Chem. Phys., 18, 4557-4568, 10.1039/C5CP06446E, 2016.

Liu, J., Fang, S., Wang, Z., Yi, W., Tao, F. M., and Liu, J. Y.: Hydrolysis of sulfur dioxide in small clusters of sulfuric acid: mechanistic and kinetic study, Environ. Sci. Technol., 49, 13112-13120, 10.1021/acs.est.5b02977, 2015

Long, B., Bao, J. L., and Truhlar, D. G.: Atmospheric chemistry of Criegee intermediates: unimolecular reactions and reactions with water, J. Am. Chem. Soc., 138, 14409-14422, 10.1021/jacs.6b08655, 2016.

Mendes, J., Zhou, C. W., and Curran, H. J.: Theoretical chemical kinetic study of the H-atom abstraction reactions from aldehydes and acids by H atoms and OH, HO_2, and CH_3 radicals, J. Phys. Chem. A, 118, 12089-12104, 10.1021/jp5072814, 2014.

Novelli, A., Hens, K., Ernest, C. T., Martinez, M., Nölscher, A. C., Sinha, V., Paasonen, P., Petäjä, T., Sipilä, M., Elste, T., Plass-Dülmer, C., Phillips, G. J., Kubistin, D., Williams, J., Vereecken, L., Lelieveld, J., and Harder, H.: Identifying Criegee intermediates as potential oxidants in the troposphere, Atmos. Chem. Phys. Discuss., 10.5194/acp-2016-919, 2016.

Novelli, A., Hens, K., Ernest, C. T., Martinez, M., Nölscher, A. C., Sinha, V., Paasonen, P., Petäjä, T., Sipilä, M., Elste, T., Plass-Dülmer, C., Phillips, G. J., Kubistin, D., Williams, J.,

Vereecken, L., Lelieveld, J., and Harder, H.: Estimating the atmospheric concentration of Criegee intermediates and their possible interference in a FAGE-LIF instrument, Atmos. Chem. Phys., 17, 7807-7826, 10.5194/acp-17-7807-2017, 2017.

Ryzhkov, A. B., and Ariya, P. A.: The importance of water clusters $(H_2O)_n$ (n=2, ... ,4) in the reaction of Criegee intermediate with water in the atmosphere, Chem. Phys. Lett., 419, 479-485, 10.1016/j.cplett.2005.12.016, 2006.

Taatjes, C. A., Welz, O., Eskola, A. J., Savee, J. D., Scheer, A. M., Shallcross, D. E., Rotavera, B., Lee, E. P. F., Dyke, J. M., Mok, D. K. W., Osborn, D. L., and Percival, C. J.: Direct measurements of conformer-dependent reactivity of the Criegee intermediate CH_3CHOO, Science, 340, 177-180, 10.1126/science.1234689, 2013.

Zhang, P., Wang, W. L., Zhang, T. L., Chen, L., Du, Y. M., Li, C. Y., and Lü, J.: Theoretical study on the mechanism and kinetics for the self-reaction of C2H5O2 radicals, J. Phys. Chem. A, 116, 4610-4620, 10.1021/jp301308u, 2012.